Mid-Tropospheric moisture variations during the development of hurricane Karl as resolved by airborne GPS radio occultation with open loop tracking

Brian Murphy[1] Jennifer Haase[2] Kuo-Nung Wang[3], James L. Garrison[3], Xue Meng Chen[4], Shu-Hua Chen[4], Loknath Adhikari[5], Feiqin Xie[5]

1. Department of Earth, Atmospheric and Planetary Sciences Purdue University, West Lafayette, IN 47906 2. Scripps Institution of Oceanography, UCSD, La Jolla, CA 92093 3. Astronautics and Aeronautics, Purdue University, West Lafayette, IN 47906
4. Departmant of Land, Air and Water Resources, University of California, Davis, CA 95616 5. Department of Earth and Atmospheric Sciiences, Texas A & M Corpus Christi, Corpus Christi, TX

A51A-0001

Introduction

The PRE-Depression Investigation of Cloud-systems in the Tropics (PREDICT) field campaign from 15 August to 30 September 2010 focused on developing tropical disturbances in the Caribbean and mid-Atlantic. The development of hurricane Karl in 2010 was investigated with dropsonde and airborne radio occultation (ARO) measurements from the stage of tropical disturbance with an easterly wave through to genesis of the tropical storm. Infrared imagery showed deep convection with extensive cold cloud tops on 11 September, however the storm failed to develop until 3 days later. One possible explanation is the horizontal offset of the mid and lower level circulation centers. We illustrate with airborne radio occultation measurements additional information on the moisture distribution during this stage of development that indicates that average mid-level moisture was lower the following day and then increased again over the next two days prior to development. High sample rate RF data recorded by the GNSS instrument system for multistatic and occultation sensing (GISMOS) was analyzed with a version of the Purdue Software Receiver that has open-loop tracking implemented. We retrieve slanted vertical profiles of atmospheric refractivity that can be considered a proxy for moisture in this tropical environment. We illustrate that in the mid to upper troposphere, ARO refractivity profiles sampling different areas within the tropical wave showed characteristics that were consistent with (~150 to 200 km scale) horizontal moisture gradients present in the NWP model representation of the developing tropical storm. Variation in refractivity preceding the development of the pre-Karl system is consistent with increasing moisture near the storm center. The ARO observations almost double the amount of thermodynamic data over that provided by the dropsondes. They provide interesting complementary measurements that sample regions off the flight path.

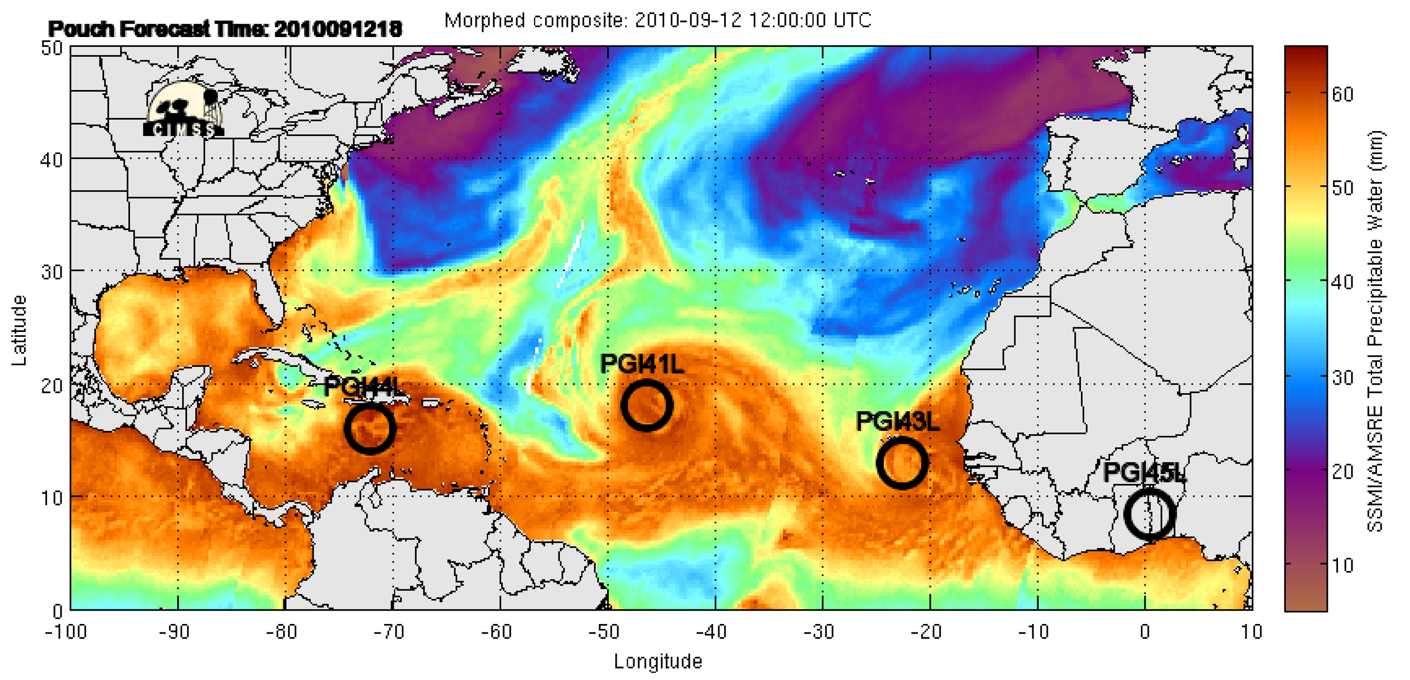

PREDICT Campaign: Tropical disturbances moving with African Easterly Waves (AEW) across the central Atlantic and into the Caribbean were identified as potential targets for study. While most of these disturbances do not develop, the majority of Atlantic hurricanes originate from cloud systems associated with AEW [Landsea, 1993].

Atmospheric Refractivity Measured by ARO

GPS radio occultation is used to remotely sense the atmosphere in all weather conditions and retrieve high resolution profiles of atmospheric refractivity. The observed delay of GPS signals propagating through the atmosphere compared to vacuum is used to obtain atmospheric refractivity. The signals are tracked as a transmitting GPS satellite sets below or rises above the horizon. The ray path is characterized by its tangentpoint, which is the point of closest approach to the Earth's surface. The tangent point of the ray path is important in that most of the bending due to refraction occurs in the vicinity of the tangent point. [Kursinski et al 1997] The location of the tangent point drifts away from or towards the location of the aircraft as the occulting satellite sets or rises. Typically this drift is ~300-500 km.

$$N = k_1\frac{P}{T} - k_2'\frac{e}{T} + k_3\frac{e}{T^2};\quad N = (n-1)\times 10^6$$

Atmospheric refractivity is directly related to pressure,, temperature , and water vapor pressure as shown in the above relation. The dependence of refractivity on atmospheric variables can be separated into 'wet' terms with moisture dependence and a 'dry' term. Vertical temperature profiles in tropical regions are relatively homogeneous and variation of refractivity below 8 km altitude is due primarily to moisture variation. Therefore, refractivity serves as a first order proxy for moisture. We define a background environmental mean profile for Karl as the average of all dropsonde measurements (shown on the right) recorded during flights RF14-RF18.

Pre-Karl Dropsonde Refractivity

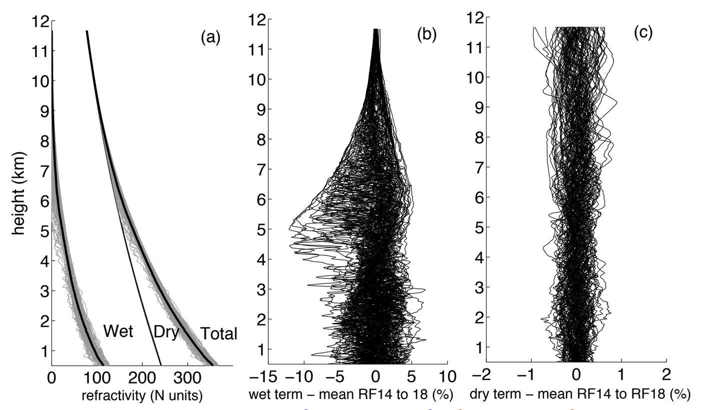

$$N = k_2'\frac{e}{T} + k_3\frac{e}{T^2} + k_1\frac{P}{T}$$

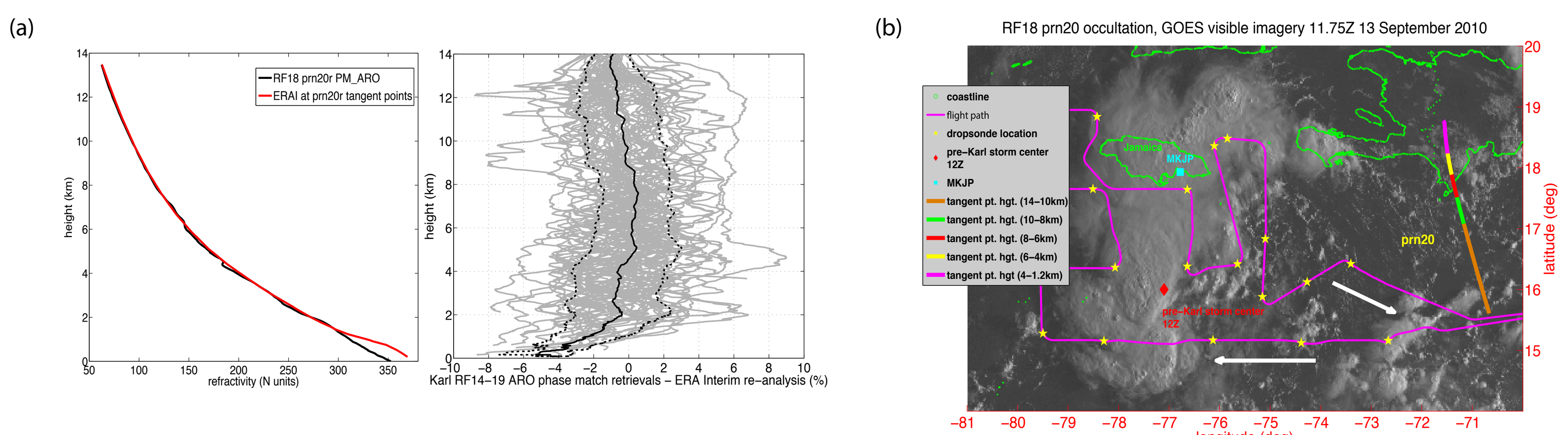

(a) A comparison of the ARO refractivity profile with the ERA Interim re-analysis for Research Flight (RF) 18 shows 2% error on average. The ARO refractivity was obtained from measurements using occulting GPS prn20 satellite using a radio-holographic phase matching technique [Jenson et al. 2004; Wang et al. 2016]. ERA-I comparison points were calculated from refractivity at the prn20 tangent point heights and positions.

(b) The flight path of RF18 is shown overlaid on the 11:45 (UT) GOES-13 visible imagery. The prn20 tangent point location drift is illustrated through succeeding height intervals.

Pre-Karl Development

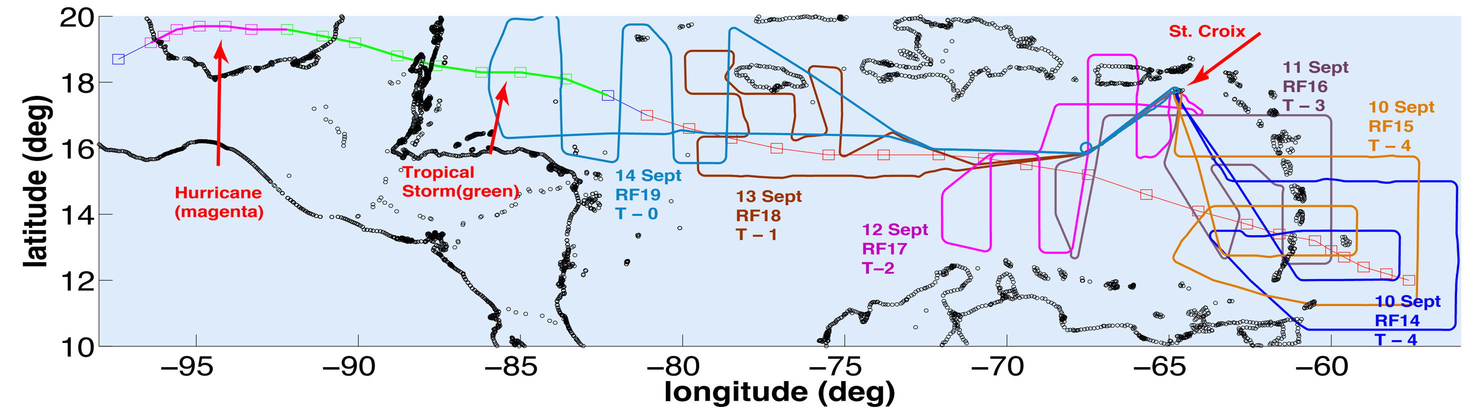

The pre-Karl disturbance initially formed from a merger of an easterly wave and a low pressure trough over the north Atlantic coast of Venezuela about 8 September 2010. The system exhibited a diurnal convection pattern as it moved slowly across the Caribbean over 10 -13 September. The system entered the Caribbean with mis-aligned mid and lower level circulation centers [Davis and Ahijevych, 2012] which may have delayed development. The disturbance reached tropical depression strength on 14 September (day T - 0) and after continued rapid development became a major hurricane in the Bay of Campeche by 17 September.

ARO Meso-α Refractivity Measurements

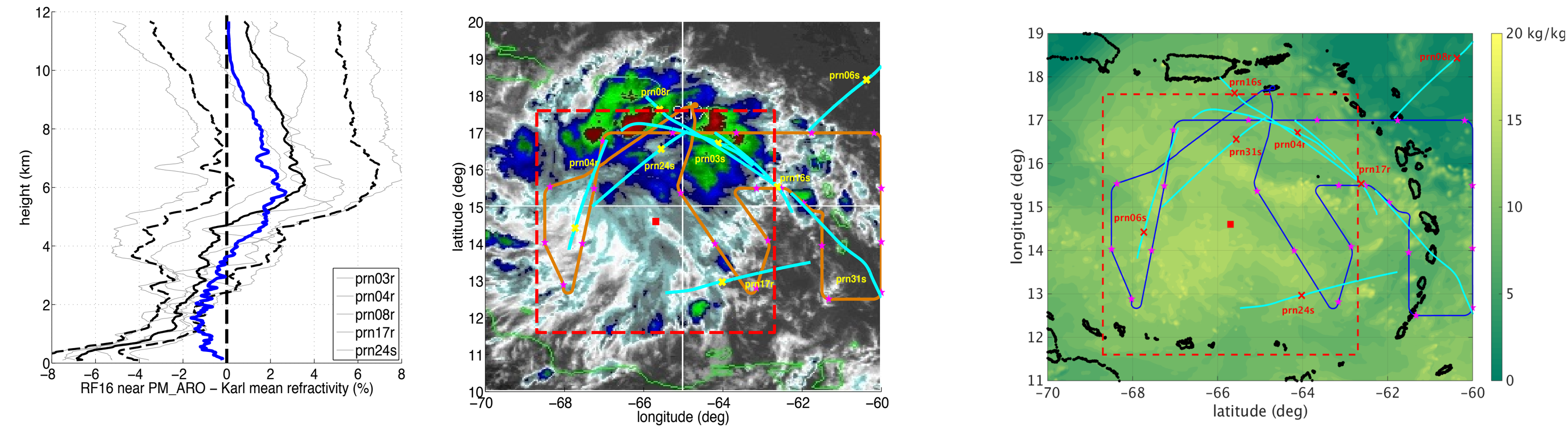

RF16: A near storm meso-α region has been defined as a 6 x 6 degree box centered on the National Hurricane Center best track locations. Occultation point locations (defined as 500 hPa height tangent point) inside the region are included in the near storm average. LEFT: the RF16 near storm refractivity mean minus the environmental mean profile (defined above) as a function of height is shown by solid black line while the standard deviation is shown by dashed black lines. The near storm refractivity mean calculated from dropsondes in the region is shown in blue. CENTER: The RF16 flight track is overlaid on GOES-13 ch4 thermal infrared imagery. ARO tangent point paths are drawn in cyan with occultation points indicated by yellow crosses. Dropsonde locations are marked by magenta stars. The meso-α region is shown by the dashed red box. RIGHT: The mid-tropospheric column precipitable water from 4 - 8 km altitude calculated from a high resolution Weather and Research Forecasting (WRF) model simulation which assimilated PREDICT dropsondes. The RF16 flight path is plotted with dropsondes indicated by magenta stars and ARO tangent point paths drawn in cyan. Occultation points are marked by red crosses

After a strong pulse of convection, the ARO mean near storm refractivity indicated a moist mid-troposphere (4 - 8 km) relative to the environmental mean refractivity.

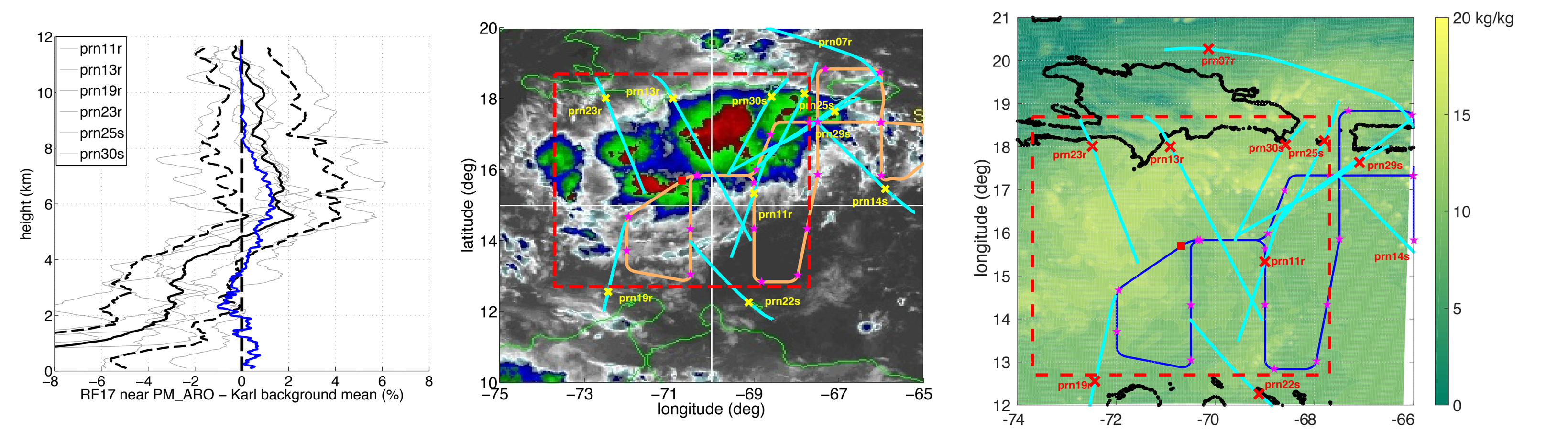

RF17: LEFT, CENTER and RIGHT figures same as RF16 above.

During RF17 dropsondes could not be deployed near the area of strongest convection due to hazardous flight conditions. However, the region was sampled by ARO. The meso-α mean refractivity was lessened from RF16. The development may have been inhibited by the continued mis-alignment of the surface and mid-level circulation centers.

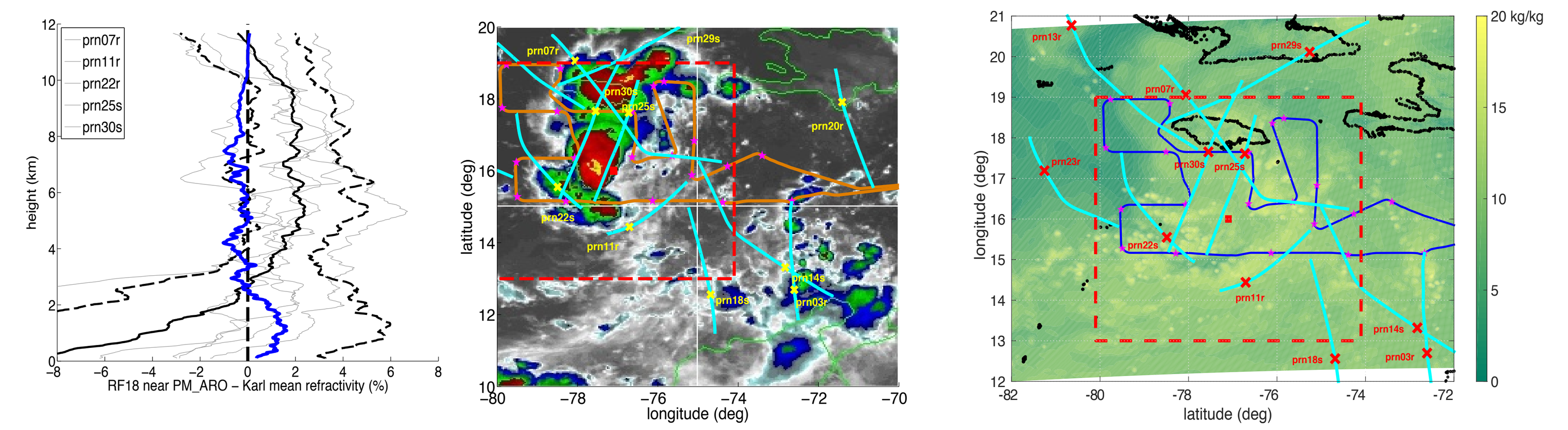

RF18: Upper LEFT, CENTER and RIGHT figures same as RF16 above.

Several dropsondes to the north and west of the storm center, as well as to the east. sampled outlying dryer regions. ARO was able to sample more of the high moisture regions in the extended area of convection along a northeast line near the storm center. RF18 ARO results provide important additional data on the increased mid to upper tropospheric moistening that can be used to help accurately forecast the development of the pre-Karl disturbance.

Acknowledgements

Xue Meng Chen and Shu-Hua Chen provided high resolution WRF simulation runs that assimilated all PREDICT dropsonde data. This work was funded bycontributions from the following grants: HIAPER UCAR Subcontract S05-39696, NSF grant SGER-0802887, NSF grant AGS 1015904, NSF grant AGS 1301835, NASA grant NNX12AK30G. ERAI reanalyses were provided by the European Center for Medium Range Forecasts (ECMWF), http://apps.ecmwf.int/datasets/, and PREDICT dropsonde data were provided by NCAR-EOL, http://data.eol.ucar.edu/master_list/?project=PREDICT. GOES imagery was obtained for the PREDICT field catalog, http://catalog.eol.ucar.edu/predict/.
The analyzed refractivity profiles are available at the webpage, http://www.igpppublic.ucsd.edu/~jhaase/airborne_ro.

References

Chen, Xue Meng and Shu-Hua Chen, (2016) NSF Final Technical Report, "Collaborative Research: Investigating the Characteristics of Lower Tropospheric Airborne GPS Radio Occultation Observations and Their Impact in Hurricane Studies".
Davis, C. A., and D. A. Ahijevych (2012), Mesoscale structural evolution of threetropical weather systems observed during PREDICT, J. Atmos. Sci., 69(4), 1284-1305, doi:10.1175/jas-d-11-0225.1.
Jensen, A. S., M. S. Lohmann, A. S. Nielsen, and H. H. Benzon (2004), Geometrical optics phase matching of radio occultation signals, Radio Sci., 39(3), doi:10.1029/2003rs002899.
Kursinski, E. R., G. A. Hajj, K. R. Hardy, J. T. Schofield, and R. Linfield (1997), Observing Earth's atmosphere with radio occultation measurements, J. Geoph.Res., 102(23), 23.429 - 423.465.
Murphy, B. J., Haase, J. S., Muradyan, P., Garrison, J. L. and Wang, K. -N. (2015), Airborne GPS radio occultation refractivity profiles observed in tropical storm environments. J. Geophys. Res. Atmos., 120: 1690–1709. doi: 10.1002/2014JD022931.
Wang et al., Implementation of the phase matching (PM) method for the GPS airborne radio occultation (ARO) system, to be submitted to J. Geophys. Res. Atmos., 2016.

ARO Refractivity: Spatial Variability

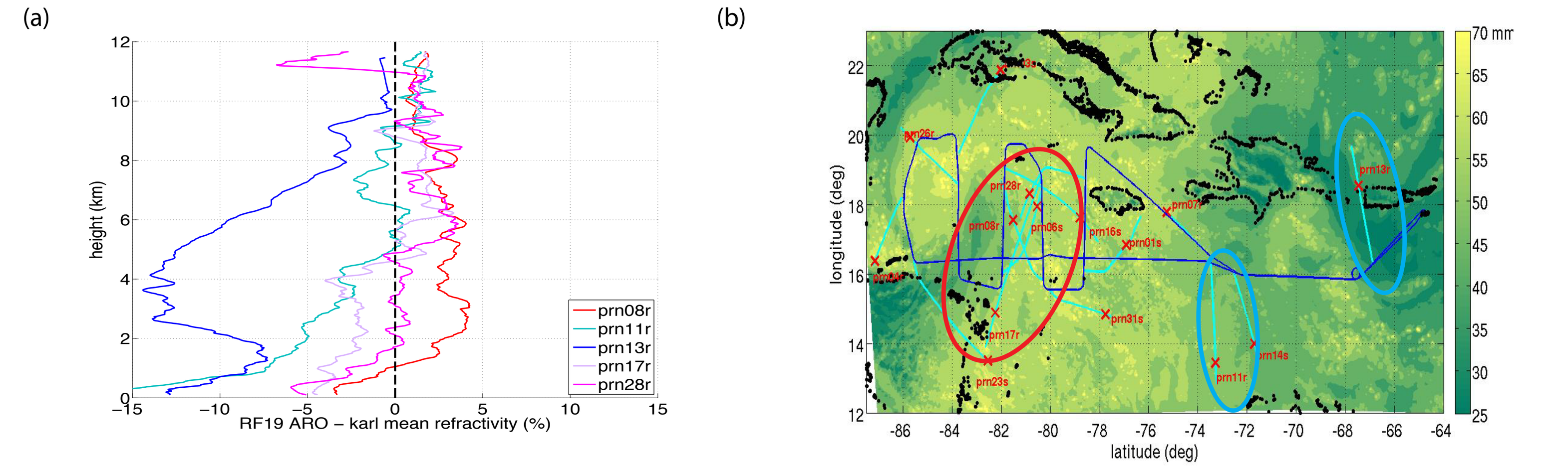

(a) Difference of RF19 ARO refractivity profiles from the Karl environmental mean refractivity.

(b) RF19 flight path overlaid on total column precipitable water calculated from a high resolution WRF simulation which assimilated dropsondes. ARO tangent point paths are shown in cyan and occultation points are marked by red crosses.

In the tropical environment, refractivity is a useful first order proxy for moisture, indicating regions of moist and dry air. For example, ARO refractivity retrievals (prn11 and prn13) sampled areas of dry air far from the storm center and show lower refractivity in the mid troposphere compared to the Karl environmental mean background. ARO retrievals (prn08, prn17, prn28) near the storm center and in moist air show higher mid-tropospheric refractivity than background.

ARO Refractivity: Spatial Resolution

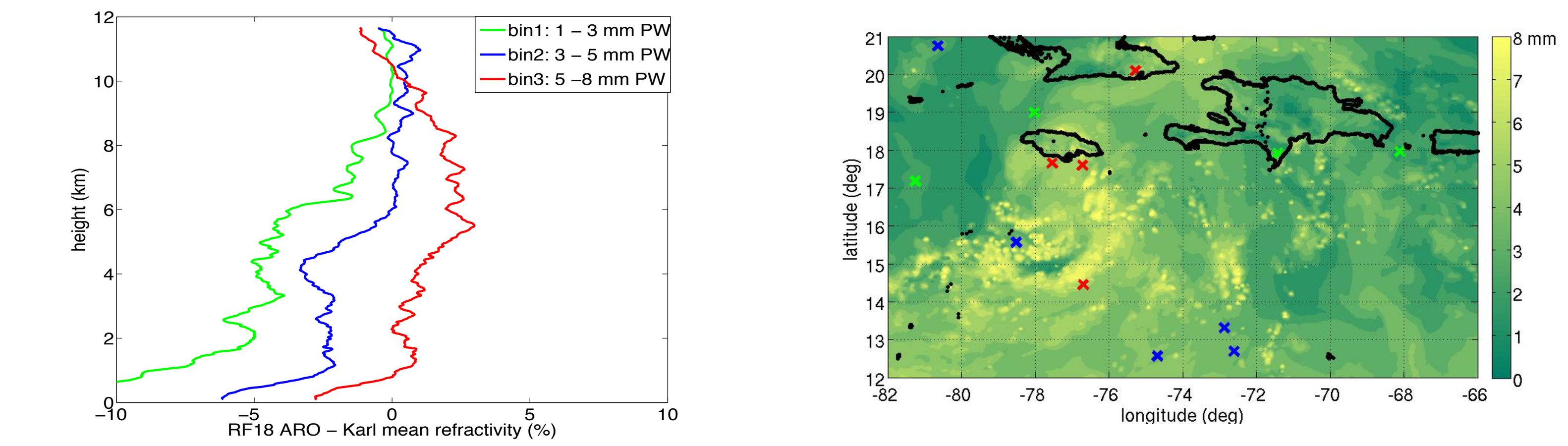

Total column precipitable water above 6 km for RF18 was calculated from a high resolution WRF simulation which assimilated PREDICT dropsondes. ARO retrievals were sorted into three bins according to the magnitude of precipitable water in the region sampled by the occultation points.

(a) Mean refractivity of RF18 retrievals for each bin.

(b) RF18 flight path overlaid on total column precipitable water above 6 km. Occultation points of each ARO retrieval are plotted and color coded to their bins.

The ARO observations, despite their large horizontal footprint, are capable of distinguishing larger scale variations of moisture on the order of about 150-200 km, represented by the binned high, mid, and lower PW values.

Preliminary ARO Assimilation Result

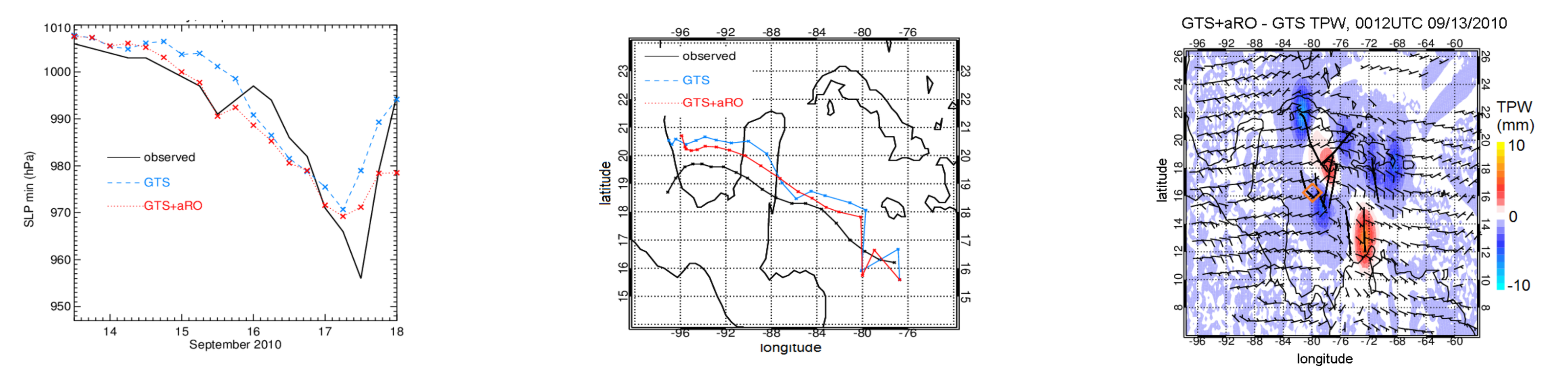

As a preliminary test of potential ARO impact on a numerical weather forecast, RF18 ARO refractivity was assimilated with Global Telecommunications System (GTS) data into a WRF simulation and compared to the assimilation of GTS only.

LEFT: ARO + GTS forecast of storm intensity matched observations more closely than GTS alone.

CENTER: ARO + GTS storm track was also improved compared with GTS alone forecast.

RIGHT: Difference between ARO + GTS and GTS alone total precipitable water (TPW) for RF18, 12Z. Wind barbs indicate the mean flow. The ARO + GTS indicate increased moisture just southeast and northwest of storm center, approximately where ARO prn25, 30 and 11 sampled, potentially contributing to improved intensity forecast. Further study indicated the increased moisture was mostly at mid-troposphere level.

Conclusions

- Under the tropical atmospheric conditions encountered during the PREDICT campaign, atmospheric refractivity is a useful first order proxy for moisture.
- ARO refractivity profiles, which the environment on both sides of the flight track, provide a valuable complement to data provided by dropsonde soundings directly beneath the aircraft. When assimilated, this additional ARO data can potentially have additional positive impact on numerical weather prediction forecasts, especially when ARO measures areas of convection not well sampled by dropsondes.
- ARO refractivity profiles from PREDICT distinguish first order spatial variations in moisture.
- Regions of moisture variation on the order of 150 – 200 km could be resolved by the mean ARO refractivity retrieved over those regions.